

# Quinoline-Based Fluorescent Probe for Ratiometric Detection of Lysosomal pH

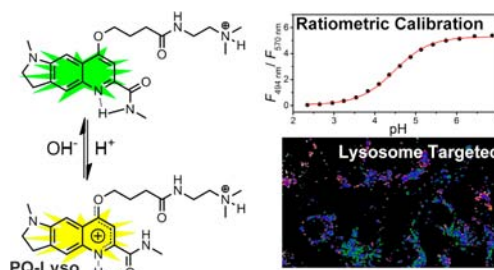
Guoping Li,<sup>†</sup> Dongjian Zhu,<sup>†</sup> Lin Xue,<sup>†,\*</sup> and Hua Jiang<sup>\*,†,‡</sup>

Beijing National Laboratory for Molecular Sciences, CAS Key Laboratory of Photochemistry, Institute of Chemistry, Chinese Academy of Sciences, Beijing 100190, P. R. China, and College of Chemistry, Beijing Normal University, Beijing 100875, P. R. China

hjiang@iccas.ac.cn; zinclin@iccas.ac.cn

Received August 16, 2013

## ABSTRACT



A new pH-responsive fluorescent probe has been reported based on protonation-activable resonance charge transfer. In aqueous solution, probe PQ-Lyso exhibits ratiometric detection of pH changes with a large hypsochromic shift of 76 nm and remarkable changes in the fluorescence intensity ratio ( $R = F_{494\text{ nm}}/F_{570\text{ nm}}$ ,  $R/R_0 = 105$ ). Furthermore, PQ-Lyso, which is localized to lysosomes in living cells, can calibrate lysosomal pH using fluorescence ratiometry.

Intracellular pH, known as  $\text{pH}_i$ , plays a critical role in living cells.<sup>1</sup> Numerous metabolic pathways require stringent regulation of the  $\text{pH}_i$ . Remarkably, the pH within lysosomes is maintained at 4.5–5.5, providing the basic requirement for the action of lysosomal hydrolases to degrade proteins, DNA, RNA, polysaccharides, and lipids.<sup>2</sup> Disruptive variation in the lysosomal pH causes defects in lysosomal function and consequently leads to many lysosomal storage diseases.<sup>3</sup> Recent evidence also reveals that lysosomal pH is also connected with ion metabolism and oxidative stress.<sup>4</sup> Therefore, it is important

to track lysosomal pH in living cells to understand its physiological and pathological processes.

Fluorescent microscopy is becoming one of the most powerful tools for monitoring intracellular species because of its high spatial and temporal resolution.<sup>5</sup> In particular, the ratiometric fluorescence technique, in principle providing quantitative measurements, is regarded as an ideal method for accessing intracellular pH.<sup>6</sup> Although considerable endeavors have been devoted to the development of pH-responsive ratiometric probes based on small molecules,<sup>7</sup>

<sup>†</sup> Institute of Chemistry, Chinese Academy of Sciences.

<sup>‡</sup> Beijing Normal University.

- (1) (a) Busa, W.; Nucitelli, R. *Am. J. Physiol.* **1984**, *246*, R409–R438. (b) Busa, W. *Annu. Rev. Physiol.* **1986**, *48*, 389–402. (c) Casey, J. R.; Grinstein, S.; Orłowski, J. *Nat. Rev. Mol. Cell Biol.* **2010**, *11*, 50–61. (2) Luzio, J. P.; Pryor, P. R.; Bright, N. A. *Nat. Rev. Mol. Cell Biol.* **2007**, *8*, 622–632. (3) Fukuda, T.; Ewan, L.; Bauer, M.; Mattaliano, R. J.; Zaal, K.; Ralston, E.; Plotz, P. H.; Raben, N. *Ann. Neurol.* **2006**, *59*, 700–708. (4) (a) Christensen, K. A.; Myers, J. T.; Swanson, J. A. *J. Cell Sci.* **2002**, *115*, 599–607. (b) DiCiccio, J. E.; Steinberg, B. E. *J. Gen. Physiol.* **2011**, *137*, 385–390. (c) Lee, S. J.; Cho, K. S.; Koh, J. Y. *Glia* **2009**, *57*, 1351–1361. (d) Lee, S. J.; Park, M. A.; Kim, H. J.; Koh, J. Y. *Glia* **2010**, *58*, 1186–1196. (e) Lockwood, T. D. *Metallomics* **2013**, *5*, 110–124.

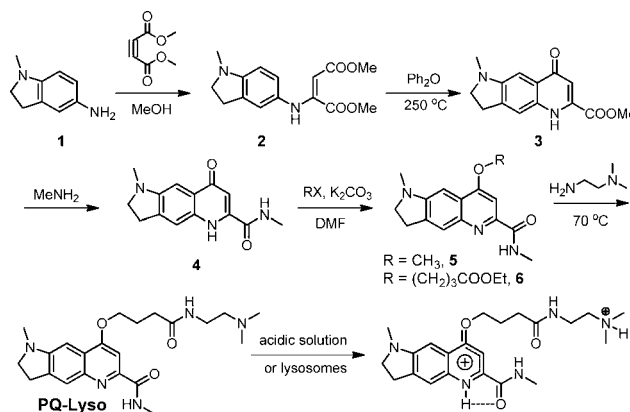
- (5) (a) Jiang, P. J.; Guo, Z. J. *Coord. Chem. Rev.* **2004**, *248*, 205–229. (b) Kikuchi, K.; Komatsu, K.; Nagano, T. *Curr. Opin. Chem. Biol.* **2004**, *8*, 182–191. (c) Lim, M. H.; Lippard, S. J. *Acc. Chem. Res.* **2007**, *40*, 41–51. (d) Domaille, D. W.; Que, E. L.; Chang, C. J. *Nat. Chem. Biol.* **2008**, *4*, 168–175. (e) Chen, X.; Tian, X.; Shin, I.; Yoon, J. *Chem. Soc. Rev.* **2011**, *40*, 4783. (f) Vendrell, M.; Zhai, D.; Er, J. C.; Chang, Y.-T. *Chem. Rev.* **2012**, *112*, 4391–4420. (6) Han, J.; Burgess, K. *Chem. Rev.* **2010**, *110*, 2709–2728. (7) (a) Wang, R.; Yu, C.; Yu, F.; Chen, L. *Trends Anal. Chem.* **2010**, *29*, 1004–1013. (b) Chen, S.; Hong, Y.; Liu, Y.; Liu, J.; Leung, C. W. T.; Li, M.; Kwok, R. T. K.; Zhao, E.; Lam, J. W. Y.; Yu, Y.; Tang, B. *J. Am. Chem. Soc.* **2013**, *135*, 4926–4929. (c) Basabe-Desmonts, L.; Reinhoudt, D. N.; Crego-Calama, M. *Chem. Soc. Rev.* **2007**, *36*, 993–1017. (d) Yuan, L.; Lin, W.; Cao, Z.; Wang, J.; Chen, B. *Chem.—Eur. J.* **2012**, *18*, 1247–1255. (e) Myochin, T.; Kiyose, K.; Hanaoka, K.; Kojima, H.; Terai, T.; Nagano, T. *J. Am. Chem. Soc.* **2011**, *133*, 3401–3409.

nanoparticles,<sup>8</sup> and polymers,<sup>9</sup> only a limited number of them have been applied to subcellular labeling and pH sensing.<sup>10</sup> Thus, it is still challenging to contribute molecular tools for subcellular pH quantification.

Our previous studies demonstrated that quinoline derivatives are useful fluorophores to design fluorescent probes because the analyte can affect the photophysical state of the fluorophore through direct coordination with quinolinic nitrogen atom. We recently introduced a class of 4-substituted, 6-dimethylquinoline-based ratiometric probes.<sup>11</sup> In aqueous medium, protonation-activable resonance charge transfer (PARCT) from the 4-position electron-donating group to the quinolinic nitrogen takes place leading to charge delocalization and significant red-shift in both absorption and emission wavelength. These observations encouraged us to make use of such PARCT process to design pH-responsive ratiometric probes based on quinoline derivatives. However, the pH-responsive spectra changes of reported probes demonstrate the UV-excitation of unprotonated compounds diminished the ratiometric signal output and potentially limited the cellular application.<sup>11a</sup>

To address this issue, it is imperative to build a new sensing platform. First, we introduced a weak electron-withdrawing acetamido instead of alkyl group at the 2-position of quinoline. This would not only enhance the charge-transfer process but also import a diverse proton receptor. Second, it is acknowledged that restricting the intramolecular rotation causes the restriction of the non-radiative pathway and reduction of twisted intramolecular charge transfer (TICT) state, consequently improving quantum yield of the fluorophore.<sup>12</sup> Last, the attachment of a basic dimethylethylamino moiety, as the lysosome anchor, to the tail of the 4-position on quinoline fluorophore would cause the accumulation of the probe in the acidic lysosomes, because of the protonation of the dimethylethylamino moiety. Therefore, we here reported the design, synthesis, and photophysical evaluation of the

**Scheme 1.** Synthesis of Compounds



probe **PQ-Lyso** in aqueous buffer and subcellular pH calibration.

The synthetic procedures of **PQ-Lyso** were shown in Scheme 1. Reaction of 1-methylindolin-5-amine (**1**) with dimethyl acetylenedicarboxylate in methanol afforded compound **2**, which was converted into quinolinone **3** in reflux of Ph<sub>2</sub>O. Further amidation of **3** using methylamine can afford **4** in a high yield. Compounds **5** and **6** were then obtained by direct alkylation of **4** with the corresponding haloalkanes. Aminolysis of **6** was performed to produce **PQ-Lyso** in an acceptable yield. These compounds were characterized by <sup>1</sup>H NMR, <sup>13</sup>C NMR, and high-resolution mass spectra analysis (see the Supporting Information).

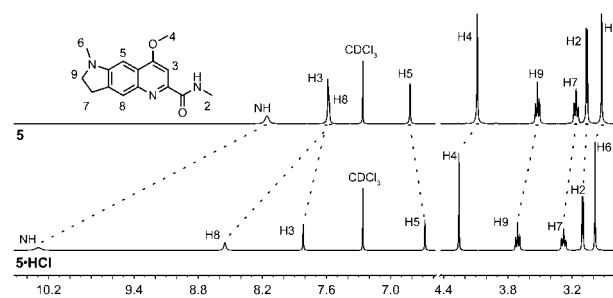


**Figure 1.** Partial <sup>1</sup>H NMR spectra of **5** (10 mM) and **5·HCl** (10 mM) in CDCl<sub>3</sub>.

At first, we prepared the control compound **5** and its protonated form of **5·HCl**<sup>13</sup> to study the proton-binding behavior by <sup>1</sup>H NMR spectroscopy. The assignments of the proton signals are based on NOE experiments (Figure S1, Supporting Information). As shown in Figure 1, upon protonation the quinolinic protons of **5** (H3 and H8) displayed significant downfield shifts of 0.23 and 0.98 ppm, respectively, suggesting that the protonation occurred at the quinolinic site. The amide proton (NH) also underwent

(8) (a) Shi, W.; Li, X.; Ma, H. *Angew. Chem., Int. Ed.* **2012**, *51*, 6432–6435. (b) Peng, H. S.; Stolwijk, J. A.; Sun, L. N.; Wegener, J.; Wolfbeis, O. S. *Angew. Chem. Int. Ed.* **2010**, *49*, 4246–4249. (c) Marin, M. J.; Galindo, F.; Thomas, P.; Russell, D. A. *Angew. Chem., Int. Ed.* **2012**, *51*, 9657–9661. (d) Benjaminsen, R. V.; Sun, H.; Henriksen, J. R.; Christensen, N. M.; Almdal, K.; Andresen, T. L. *ACS Nano* **2011**, *5*, 5864–5873.

(9) Albertazzi, L.; Storti, B.; Marchetti, L.; Beltram, F. *J. Am. Chem. Soc.* **2010**, *132*, 18158–18167.

(10) (a) Ji, J.; Rosenzweig, N.; Griffin, C.; Rosenzweig, Z. *Anal. Chem.* **2000**, *72*, 3497–3503. (b) Lee, M.; Gubernator, N. G.; Sulzer, D.; Sames, D. *J. Am. Chem. Soc.* **2010**, *132*, 8828–8830. (c) Sun, H.; Almdal, K.; Andresen, T. L. *Chem. Commun.* **2011**, *47*, 5268–5270. (d) Wu, S.; Li, Z.; Han, J.; Han, S. *Chem. Commun.* **2011**, *47*, 11276–11278. (e) Park, H. J.; Lim, C. S.; Kim, E. S.; Han, J. H.; Lee, T. H.; Chun, H. J.; Cho, B. R. *Angew. Chem., Int. Ed.* **2012**, *51*, 2673–2676. (f) Lee, M. H.; Han, J. H.; Lee, J. H.; Park, N.; Kumar, R.; Kang, C.; Kim, J. S. *Angew. Chem., Int. Ed.* **2013**, *52*, 6206–6209.

(11) (a) Xue, L.; Li, G. P.; Liu, Q.; Wang, H. H.; Liu, C.; Ding, X. L.; He, S. G.; Jiang, H. *Inorg. Chem.* **2011**, *50*, 3680–3690. (b) Wang, H. H.; Xue, L.; Jiang, H. *Org. Lett.* **2011**, *13*, 3844–3877. (c) Xue, L.; Li, G. P.; Yu, C. L.; Jiang, H. *Chem.—Eur. J.* **2012**, *18*, 1050–1054. (d) Xue, L.; Li, G.; Zhu, D.; Liu, Q.; Jiang, H. *Inorg. Chem.* **2012**, *51*, 10842–10849.

(12) (a) Grabowski, Z. R.; Rotkiewicz, K. *Chem. Rev.* **2003**, *103*, 3899–4031. (b) Everett, R. K.; Nguyen, H. A.; Abelt, C. J. *J. Phys. Chem. A* **2010**, *114*, 4946–4950. (c) Hong, Y.; Lam, J. W.; Tang, B. Z. *Chem. Commun.* **2009**, 4332–4353.

(13) The hydrochlorate salt was prepared by reaction of **5** with 1 M HCl in ethanol.

a significant downfield shift from 8.16 to 10.30 ppm ( $\Delta\delta = 2.14$  ppm), whereas acetyl proton (H2) displayed a slight downfield shift of 0.04 ppm. These data clearly demonstrate that the carbonyl oxygen atom took part in coordination with the proton. Moreover, methoxyl proton (H4) downfield shifted from 4.08 to 4.26 ppm ( $\Delta\delta = 0.18$  ppm), indicating delocalization of the positive charge on the oxygen atom. These results coincide with our previous reports and confirm the existence of resonance charge transfer from methoxyl oxygen atom to quinolinic nitrogen atom.<sup>11a</sup>

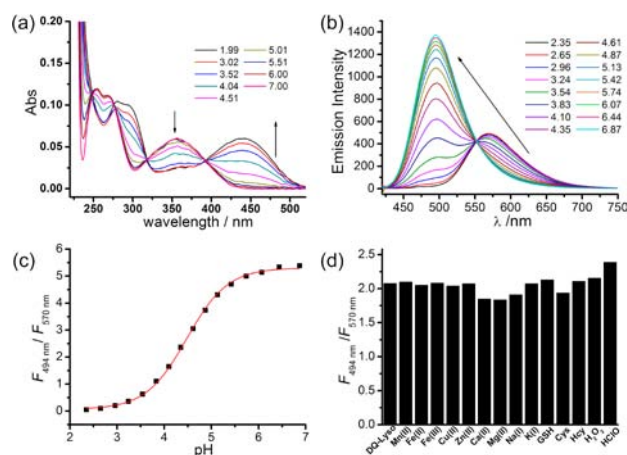


**Figure 2.** (a) Absorption spectra of **PQ-Lyso** (5  $\mu$ M). (b) Fluorescence emission spectra of **PQ-Lyso** (2  $\mu$ M) in  $\text{Na}_2\text{HPO}_4$ –citrate buffer (10 mM  $\text{Na}_2\text{HPO}_4$  and 10 mM citric acid) at various pH values. (c) Ratio ( $F_{494 \text{ nm}}/F_{570 \text{ nm}}$ ) changes as a function of the pH values. (d) Emission spectra of **PQ-Lyso** (2  $\mu$ M) in the presence of various metal ions (100  $\mu$ M  $\text{Mn}^{2+}$ ,  $\text{Fe}^{3+}$ ,  $\text{Fe}^{2+}$ ,  $\text{Cu}^{2+}$ ,  $\text{Zn}^{2+}$ , and 1 mM  $\text{Mg}^{2+}$ ,  $\text{Ca}^{2+}$ ,  $\text{Na}^+$ , and  $\text{K}^+$ ), 5 mM thiols (GSH, Cys, Hcy), and 100  $\mu$ M  $\text{H}_2\text{O}_2$  and NaClO in  $\text{Na}_2\text{HPO}_4$ –citrate buffer (pH = 4.2).  $\lambda_{\text{ex}} = 405$  nm.

To evaluate the optical response of **PQ-Lyso** to pH in aqueous solution, we measured the water solubility of the probe in  $\text{Na}_2\text{HPO}_4$ –citrate buffer. **PQ-Lyso** can be dissolved well in aqueous buffers (Figure S2, Supporting Information). As shown in Figure 2a, **PQ-Lyso** displays an obvious absorption band around 400–500 nm ( $\epsilon = 8.69 \times 10^3 \text{ M}^{-1} \text{ cm}^{-1}$ , at 405 nm, pH = 1.99) in acidic media. Up-regulation of pH induced gradual decrease of this band and appearance of a new band around 300–400 nm with several isosbestic points at 248, 276, 318, and 392 nm (Figure 2a). As expected, upon excitation at 405 nm, **PQ-Lyso** showed a remarkable fluorescence emission at 570 nm with a high quantum yield of 0.26 under acidic conditions (Figure 2b). Compared with that of reported **DQZns** and **DQCs** probes,<sup>11</sup> we infer that the 2-position amide group participated in charge delocalization through the proton binding, inducing red-shifted emission. The fixation of 6-position amino group apparently enhanced the luminance efficiency. Further titration of **PQ-Lyso** with NaOH caused the decrease of the emission intensity at 570 nm. Simultaneously, a new blue-shift emission

appeared at 494 nm ( $\Phi = 0.59$ ) with a large hypsochromic shift of 76 nm and a distinct isoemission point at 553 nm. The fluorescence intensity ratio ( $F_{494 \text{ nm}}/F_{570 \text{ nm}}$ ) of **PQ-Lyso** displayed a reversible variation as pH was changed repeatedly between 3.0 and 6.0 (Figure S3, Supporting Information). By plotting the fluorescence intensity ratio ( $F_{494 \text{ nm}}/F_{570 \text{ nm}}$ ) vs the probe concentration, the  $\text{pK}_a$  of **PQ-Lyso** was calculated to be  $4.20 \pm 0.015$  (Figure 2c and Figure S4, Supporting Information), which is suitable for lysosomal pH range. The extremely large ratio increase was calculated to be 105-fold ( $R_{\text{pH}6.87}/R_{\text{pH}2.35}$ ). Meanwhile, the control compound **5** displayed a  $\text{pK}_a$  of  $4.40 \pm 0.015$  (Figure S5, Supporting Information), indicating the attachment of dimethylethylamino group on the quinoline scaffold does not apparently affect the optical response of **PQ-Lyso**.<sup>11d</sup>

To further evaluate whether the ratiometric pH-responsive properties can be interfered by other biological molecules, we measured the fluorescence emission spectra in the presence of essential metal ions ( $\text{Na}^+$ ,  $\text{K}^+$ ,  $\text{Ca}^{2+}$ ,  $\text{Mg}^{2+}$ ,  $\text{Zn}^{2+}$ ,  $\text{Mn}^{2+}$ ,  $\text{Cu}^{2+}$ ,  $\text{Fe}^{2+}$ ,  $\text{Fe}^{3+}$ ), thiols (GSH, Cys, Hcy), and reactive oxygen species ( $\text{H}_2\text{O}_2$ , HClO) in the buffer solution (pH = 4.2, 25  $^\circ\text{C}$ ), in which **PQ-Lyso** should be partially protonated. As expected, these species exerted small ratio changes (Figure 2d), indicating that **PQ-Lyso** could be used for the ratiometric detection of pH without the potential influence from intracellular biological species.

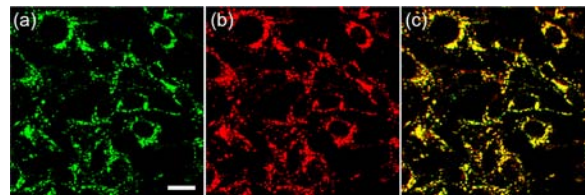


**Figure 3.** **PQ-Lyso** was localized to lysosomes in live NIH 3T3 cells. The cells were costained with (a) 2  $\mu$ M **PQ-Lyso** and (b) 0.5  $\mu$ M LysoTracker Red at 37  $^\circ\text{C}$  for 30 min in serum-free DMEM. (c) Overlay of (a) and (b). Scale bar: 20  $\mu$ m.

Next we applied **PQ-Lyso** in living cells. The NIH 3T3 cells were costained with **PQ-Lyso** and LysoTracker Red DND-99, which is a commercially available marker for lysosomes (Figure 3). The fluorescence image patterns and a Pearson's colocalization coefficient of 0.81 demonstrated that the probe can be efficiently localized to lysosomes, as observed in other probes with a similar lysosome-targeting moiety.<sup>11d,14</sup>

With these data in hand, we speculate that our ratiometric and targetable probe is a useful tool for subcellular pH imaging and quantification. For this, the in situ  $\text{pK}_a$  of **PQ-Lyso** was calibrated according to known procedures.<sup>8a,10b,f</sup> NIH 3T3 cells were incubated in a series of

(14) (a) Son, J. H.; Lim, C. S.; Han, J. H.; Danish, I. A.; Kim, H. M.; Cho, B. R. *J. Org. Chem.* **2011**, 76, 8113–8116. (b) Kim, H. M.; An, M. J.; Hong, J. H.; Jeong, B. H.; Kwon, O.; Hyon, J. Y.; Hong, S. C.; Lee, K. J.; Cho, B. R. *Angew. Chem., Int. Ed.* **2008**, 47, 2231–2234.



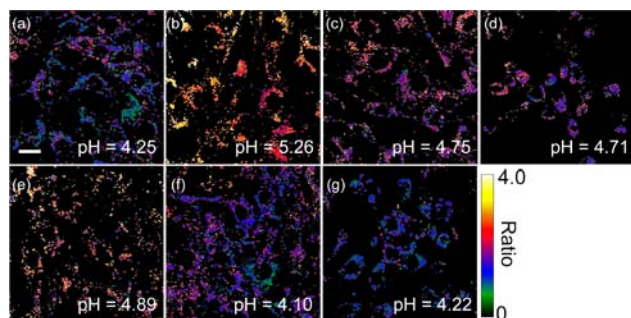


**Figure 4.** Ratiometric imaging of NIH 3T3 cells. The cells were incubated with **PQ-Lyso** (2  $\mu$ M) at 37  $^{\circ}$ C for 30 min and then treated with (a) PBS at 25  $^{\circ}$ C for 3 min, (b) 10 mM  $\text{NH}_4\text{Cl}$  at 25  $^{\circ}$ C for 1 min, (c) 50  $\mu$ M chloroquine at 25  $^{\circ}$ C for 3 min, (d) 100  $\mu$ M  $\text{H}_2\text{O}_2$  at 25  $^{\circ}$ C for 30 min, (g) 100  $\mu$ M  $\text{HClO}$  at 37  $^{\circ}$ C for 30 min. The cells were pretreated with (e) 100  $\mu$ M NEM and (f) 500  $\mu$ M NAC at 37  $^{\circ}$ C for 30 min then incubated with **PQ-Lyso** (2  $\mu$ M) for further 30 min. Average pH values were measured from 10 cells in (a–g) and were calculated from the ratio ( $F_{\text{green}}/F_{\text{red}}$ ) according to the intracellular calibration curve. Scale bar: 20  $\mu$ m, ratio bar: 0–4.

buffers of known pH in the presence of 5  $\mu$ M nigericin ( $\text{K}^+/\text{H}^+$  ionophore) and 5  $\mu$ M monensin ( $\text{Na}^+/\text{H}^+$  ionophore), which equilibrates the lysosomal pH with external surrounding media. Fluorescence ratiometric images were collected using a laser confocal scanning microscopy. The calibration curve was then established, and the in situ  $\text{pK}_a'$  was measured to be  $4.54 \pm 0.074$ . The lysosomal pH is calculated according to the Henderson–Hasselbalch equation (see the Supporting Information).

We further investigated the application of **PQ-Lyso** for monitoring lysosomal pH changes in cultured cells (Figure 4 and Figures S7 and S8, Supporting Information). After incubation with 2  $\mu$ M **PQ-Lyso** at 37  $^{\circ}$ C for 30 min, NIH 3T3 cells displayed obvious fluorescence at the red emission channel (520–600 nm) and the green emission channel (430–510 nm). The average ratio ( $F_{\text{green}}/F_{\text{red}}$ ) was calculated to be  $1.19 \pm 0.097$ , giving a corresponding pH value of  $4.25 \pm 0.34$  (Figure 4a). Treatment with 10 mM  $\text{NH}_4\text{Cl}$ , which can rapidly alkalify the lysosomes, induced a pH increase to  $5.26 \pm 0.33$  in 1 min (Figure 4b). Similarly, a lysosomotropic base, chloroquine, caused a pH increase to  $4.75 \pm 0.16$  (Figure 4c). These data clearly indicate that **PQ-Lyso** is capable of imaging and monitoring lysosomal pH changes using fluorescence ratiometry. Next, we take advantage of **PQ-Lyso** to evaluate the effects of redox agents.  $\text{H}_2\text{O}_2$  and other oxidative stress can trigger

redistribution of  $\text{H}^+$  from acidified organelles to cytosolic compartments through impairing the vacuolar proton pump ( $\text{H}^+/\text{ATPase}$ ), which imports  $\text{H}^+$  at the expense of ATP hydrolysis.<sup>15</sup> Oxidation induced alkalization of lysosomes and acidification of cytoplasm have also been observed in the literature.<sup>10f,15b</sup> In our experiments, we treated the cells with 100  $\mu$ M  $\text{H}_2\text{O}_2$  or *N*-ethylmaleimide (NEM) for generation of oxidative stress. The lysosomal pH apparently increased to be  $4.71 \pm 0.26$  and  $4.89 \pm 0.21$ , after treated with  $\text{H}_2\text{O}_2$  (Figure 4d) and NEM (Figure 4e), respectively. Treatment with NAC (*N*-acetylcysteine, a GSH precursor) resulted in a slight decrease of pH ( $4.10 \pm 0.31$ , Figure 4f). Interestingly, treatment with another oxidative chemical,  $\text{NaClO}$ , at 37  $^{\circ}$ C for 30 min did not cause significant pH changes ( $\text{pH} = 4.22 \pm 0.39$ , Figure 4g). Ma et al. also reported that elevated level of  $\text{HClO}$  cannot greatly increase the intracellular acidic substances.<sup>8a</sup> However, the detailed effect of  $\text{HClO}$  on intracellular pH has not been established well. We here provide another evidence that  $\text{HClO}$  do not obviously affect lysosomal pH in our case. We also anticipate that the lysosome-specific and ratiometric probe can contribute a useful molecular tool for the investigations on pH-relevant biological processes.

In summary, we designed a new fluorescent probe for pH based on protonation-activable resonance charge transfer. This probe can ratiometrically respond to pH changes with a large emission shift of 76 nm and an adaptable  $\text{pK}_a$  for lysosomes. Further experiments demonstrate that our probes can be localized to lysosomes in living cells. In terms of fluorescence ratiometry, we have successfully quantified the diverse lysosomal pH up-regulation under basic treatments or oxidative stress. We also emphasize that our design strategy is also feasible to design ratiometric probes for other subcellular compartments with well-tuned  $\text{pK}_a$ . This will lead to interesting and challenging work for us in the future.

**Acknowledgment.** We thank the National Natural Science Foundation of China (21102148, 21125205, 212210017), National Basic Research Program of China (2009CB930802, 2011CB935800), and the State Key Laboratory of Fine Chemicals, Department of Chemical Engineering, Dalian University of Technology, for financial support.

**Supporting Information Available.** Synthetic procedures, characterization of **PQ-Lyso**, additional spectroscopic data, and cellular fluorescence images. This material is available free of charge via the Internet at <http://pubs.acs.org>.

(15) (a) Wang, Y.; Floor, E. *J. Neurochem.* **1998**, *70*, 646–652. (b) Chen, C. S. *BMC Cell. Biol.* **2002**, *3*, 21.

The authors declare no competing financial interest.